Inorganic Chemistry

Article

Synthesis, Properties, and Crystal Structure of a Novel Anthracene-Bridged Molybdenum–Zinc Porphyrin Dimer

Tetsuaki Fujihara, Kiyoshi Tsuge, Yoichi Sasaki, Yasuhiro Kaminaga, and Taira Imamura*

Division of Chemistry, Graduate School of Science, Hokkaido University, Sapporo 060-0810, Japan

The synthesis and properties of novel anthracene-bridged porphyrin dimers having an oxomolybdenum(V) porphyrin unit, $H_2(DPA)[Mo^VO(OMe)]$ (**1**) and $(DPA)[Mo^VO(OMe)][Zn^{II}(MeOH)]$ (**2**), and the relevant monomer porphyrin complexes $Mo^VO(MPP)OMe$ (**3**) and $Zn^{II}(MPP)$ (**4**) are presented. An oxomolybdenum(V) unit was introduced into one of the two porphyrins in DPA to give **1**, which has a free-base porphyrin unit. By introducing a zinc(II) ion to the free-base part, a mixed-metal complex of **2** was prepared and isolated. The structure of **2** was analyzed by X-ray crystallography ($2 \cdot {}^7/_6 CH_2Cl_2$, triclinic, $P\bar{1}$ (no. 2), $a = 15.2854(12)$ Å, $b = 19.9640(15)$ Å, $c = 13.6915(12)$ Å, $\alpha = 90.968(3)°$, $\beta = 113.108(4)°$, $\gamma = 96.501(4)°$, $Z = 2$, R1 = 9.9, wR2 = 19.2). The structure of **2** demonstrated that a methanol is stably coordinated to the Zn(II) ion with the aid of a hydrogen bond to the methoxo ligand on the Mo(V) ion in the binding pocket of DPA. The electrochemical measurements of **2** suggested that the methanol was kept in the pocket of DPA in solution even at the reduced state of the molybdenum ion.

Introduction

Much attention has been paid to cofacial diporphyrins due to their reactivities with small molecules.[1] In particular, face-to-face diporphyrins attached by a rigid spacer such as anthracene (DPA), biphenylene (DPB), or *o*-phenylene (Gable type) have given unique properties.[1–10] For instance, biscobalt porphyrin dimers having rigid spacers display four-electron reactivity from dioxygen to water.[3–7] Diporphyrins containing various metal ions such as Mn,[8] Ru,[9] or Os[10] also show extremely metal-specific reactivities toward small molecules in the binding pocket between two porphyrin units. Especially, the introduction of different metal ions to diporphyrins is the most effective to give rise to singular properties that must be caused by intramolecular interactions between the two metal ions.[11–14] Very recently, in the

(1) Collman, J. P.; Wagenknecht, P. S.; Hutchison, J. E. *Angew. Chem., Int. Ed. Engl.* **1994**, *33*, 1534–1554 and references therein.

(2) Abbreviations: H₄DPA = 1,8-bis[5-(2,8,13,17-tetraethyl-3,7,12,18-tetramethylporphyrinyl)]anthracene, H₄DPB = 1,8-bis[5-(2,8,13,17-tetraethyl-3,7,12, 18-tetramethylporphyrinyl)]biphenylene, MPP = 5-phenyl-2,8,13,17-tetraethyl-3,7,12,18-tetramethylporphyrinato dianion, DPTBTMP = 5,15-diphenyl-2,8,12,18-tetra-*n*-butyl-3,7,13,17-tetramethylporphyrinato dianion, TPP = 5,10,15,20-tetraphenylporphyrinato dianion, 5-NO₂-OEP = 5-nitro-2,3,7,8,12,13,17,18-octaethylporphyrinato dianion, (DPA')⁴⁻ = anion of 1,8-bis[5-(2,8,12,18-tetrahexyl-3,7,13,17-tetramethyl-15-phenyl)porphyrin]anthracene, im = imidazolate, TBAP = tetra-*n*-butylammonium perchlorate.

(3) (a) Chang, C. K.; Liu, H. Y.; Abdalmuhdi, I. *J. Am. Chem. Soc.* **1984**, *106*, 2725–2726. (b) Liu, H.-Y.; Abdalmuhdi, I.; Chang, C. K.; Anson, F. C. *J. Phys. Chem.* **1985**, *89*, 665–670. (c) Ni, C.-L.; Abdalmuhdi, I.; Chang, C. K.; Anson, F. C. *J. Phys. Chem.* **1987**, *91*, 1158–1166.

(4) Collman, J. P.; Hutchison, J. E.; Lopez, M. A.; Tabard, A.; Guilard, R.; Seok, W. K.; Ibers, J. A.; L'Her, M. *J. Am. Chem. Soc.* **1992**, *114*, 9869–9877.

(5) Park, G. J.; Nakajima, S.; Osuka, A.; Kim, K. *Chem. Lett.* **1995**, 255–256.

(6) Le Mest, Y.; Inisan, C.; Laouenan, A.; L'Her, M.; Talarmin, J.; El Khalifa, M.; Saillard, J.-Y. *J. Am. Chem. Soc.* **1997**, *119*, 6095–6106.

(7) Chang, C. J.; Deng, Y.; Shi, C.; Chang, C. K.; Anson, F. C.; Nocera, D. G. *Chem. Commun.* **2000**, 1355–1356.

(8) (a) Naruta, Y.; Maruyama, K. *J. Am. Chem. Soc.* **1991**, *113*, 3595–3596. (b) Naruta, Y.; Sasayama, M.; Sasaki, T. *Angew. Chem., Int. Ed. Engl.* **1994**, *33*, 1839–1841.

(9) (a) Collman, J. P.; Hutchison, J. E.; Lopez, M. A.; Guilard, R.; Reed, R. A. *J. Am. Chem. Soc.* **1991**, *113*, 2794–2796. (b) Collman, J. P.; Hutchison, J. E.; Lopez, M. A.; Guilard, R. *J. Am. Chem. Soc.* **1992**, *114*, 8066–8073. (c) Collman, J. P.; Hutchison, J. E.; Ennis, M. S.; Lopez, M. A.; Guilard, R. *J. Am. Chem. Soc.* **1992**, *114*, 8074–8080. (d) Collman, J. P.; Hutchison, J. E.; Wagenknecht, P. S.; Lewis, N. S.; Lopez, M. A.; Guilard, R. *J. Am. Chem. Soc.* **1990**, *112*, 8206–8208. (e) Collman, J. P.; Wagenknecht, P. S.; Hutchison, J. E.; Lewis, N. S.; Lopez, M. A.; Guilard, R.; L'Her, M.; Bothner-By, A. A.; Mishra, P. K. *J. Am. Chem. Soc.* **1992**, *114*, 5654–5664.

(10) Collman, J. P.; Ha, Y.; Wagenknecht, P. S.; Lopez, M. A.; Guilard, R. *J. Am. Chem. Soc.* **1993**, *115*, 9080–9088.

(11) Guilard, R.; Lopez, M. A.; Tabard, A.; Richard, P.; Lecomte, C.; Brandes, S.; Hutchison, J. E.; Collman, J. P. *J. Am. Chem. Soc.* **1992**, *114*, 9877–9889.

(12) Guilard, R.; Tabard, A.; Bouhmaida, N.; Lecomte, C.; Richard, P.; Latour, J. M. *J. Am. Chem. Soc.* **1994**, *116*, 10202–10211.

(13) Guilard, R.; Brandes, S.; Tardieux, C.; Tabard, A.; L'Her, M.; Miry, C.; Gouerec, P.; Knop, Y.; Collman, J. P. *J. Am. Chem. Soc.* **1995**, *117*, 11721–11729.

(14) Collman, J. P.; Garner, J. M. *J. Am. Chem. Soc.* **1990**, *112*, 166–173.
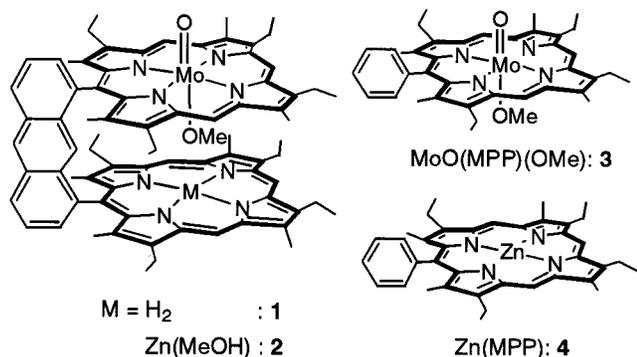
Figure 1. Anthracene-bridged porphyrin dimers having an oxomolybdenum(V) porphyrin unit and relevant monomer porphyrin complexes.

Table 1. Crystallographic Data for **2**

empirical formula	$C_{80}H_{84}N_8O_3MoZn \cdot {}^7/_6CH_2Cl_2$
temp/K	193
cryst syst	triclinic
space group	$P\bar{1}$ (No. 2)
a/Å	15.2854(12)
b/Å	19.9640(15)
c/Å	13.6915(12)
α/deg	90.968(3)
β/deg	113.108(4)
γ/deg	96.501(4)
V/Å^3	3809.5(5)
Z	2
d_{calcd}/g cm^{-3}	1.28
no. of unique reflns	16489
no. of obsd reflns	9602, $I > 2\sigma(I)$
R1,wR2, %^{a}	9.9, 19.2

^{a} R1 = $\Sigma||F_o| - |F_c||/\Sigma|F_o|$, wR2 = $\{\Sigma[w(F_o{}^2 - F_c{}^2)^2]/\Sigma[w(F_o{}^2)^2]\}^{1/2}$, $w = \{\sigma^2(F_o{}^2) + [0.03(max(F_o{}^2, 0) + 2F_c{}^2)/3]^2\}^{-1}$.

preparation of this paper, new diporphyrins of gallium–gallium, gallium–ruthenium, and gallium–cobalt DPA complexes were reported.[15] The study demonstrated that in the Ga–Ga complex an unprecedented double $\pi-\pi^*$ fluorescence was aroused from the two lowest energy absorption Q-bands and that in the Ga–Ru and Ga–Co complexes luminescences were efficiently quenched by Ru(II) and Co(II) centers.

Molybdenum in porphyrin rings can take various oxidation states from +2 to +6.[16,17] In their high oxidation states, +4, +5, and +6, the molybdenum porphyrins show a strong affinity for oxygen species and display unique photochemical and electrochemical reactivities.[18–20]

We now pay attention to heterometallic diporphyrins having a high-valent molybdenum(V) ion. Since the biphenylene spacer is short enough to form a metal–metal bond,[21] the anthracene spacer has been selected in the present study to use the binding pocket effectively. In this paper, the synthesis, characterization, and properties of novel anthracene-bridged porphyrin dimers having an oxomolybdenum(V) porphyrin unit, H$_2$(DPA)[Mo^{V}O(OMe)] (**1**) and (DPA)[Mo^{V}O(OMe)][Zn^{II}(MeOH)] (**2**), are reported (Figure 1).

Experimental Section

Methods. UV–vis spectra were recorded on a Hitachi UV-3000 spectrophotometer. IR spectra were recorded on a Hitachi 270-50 infrared spectrophotometer. ^{1}H NMR spectra were measured with a JEOL EX270 FT-NMR spectrophotometer. FAB-MS spectra and elemental analysis were carried out at the Center for Instrumental

Analysis, Hokkaido University. ESR spectra were recorded on a JEOL JES-FE3X spectrometer. Cyclic voltammograms were recorded at a scan rate of 100 mV/s with a HOKUTO DENKO HZ-3000 voltammetric analyzer. Working and counter electrodes were a Pt disk and a Pt wire, respectively. As the reference a Ag/AgCl electrode was used. The complexes (ca. 1 mM) were dissolved in CH$_2$Cl$_2$ containing 0.1 M TBAP, and the solutions were deoxygenated with a stream of argon gas.

X-ray Crystallography. The crystals of (DPA)[Mo^{V}O(OMe)]-[Zn^{II}(MeOH)] (**2**) were obtained as CH$_2$Cl$_2$ solvates (**2**$\cdot^7/_6$CH$_2$Cl$_2$). Data were collected on a Rigaku RAXIS-RAPID diffractometer with an imaging plate area detector using graphite-monochromated Mo Kα radiation ($\lambda = 0.71073$ Å) at 193 K. To determine the cell constants and the orientation matrix, two oscillation photographs were taken with an oscillation angle of 2°. Intensity data were collected by taking oscillation photographs (total oscillation range 220°, 44 frames, and exposure time 180 s). A numerical absorption correction was applied.

The crystal structure was solved by a direct method and expanded by the Fourier method. The structure was refined by full-matrix least-squares refinement on F^2. All non-hydrogen atoms of **2** were refined anisotropically. Dichloromethane molecules were inclueed as crystal solvents, which were found to be disordered and were refined isotropically. All hydrogen atoms, with the exception of those of crystal solvents, were located on the calculated positions and not refined. All calculations were performed using the teXsan crystallographic software package.[22] The crystallographic data of **2**$\cdot^7/_6$CH$_2$Cl$_2$ are summarized in Table 1.

Materials. Mo(CO)$_6$ was purchased from Aldrich. Silica gel (Wakogel C-300HG) and alumina (Woelm, neutral, activity III) were used for column chromatography. Other agents and solvents were purchased from Wako and used as received. The porphyrin ligands of H$_4$DPA[11,23] and H$_2$MPP[23] were prepared according to previous reports. The elemental analysis of each compound was satisfactory, and all the spectral data agreed well with the previous results.

H$_2$(DPA)[Mo^{V}O(OMe)] (1). H$_4$DPA (100 mg, 8.8×10^{-5} mol) and an excess of Mo(CO)$_6$ (200 mg, 7.6×10^{-4} mol) were added to the mixed solvent of decalin (36 mL) and *n*-octane (9 mL). The mixture was refluxed for 2 h under N$_2$. After the reaction mixture was filtered, the filtrate was passed through an alumina column (neutral, activity III, 2 × 10 cm). The first band eluted with neat

(15) Harvey, P. D.; Proulx, N.; Martin, G.; Drouin, M.; Nurco, D. J.; Smith, K. M.; Bolze, F.; Gros, C. P.; Guilard, R. *Inorg. Chem.* **2001**, *40*, 4142–4148.
(16) Matsuda, Y.; Murakami, Y. *Coord. Chem. Rev.* **1988**, *92*, 157–192.
(17) Brand, H.; Arnold, J. *Coord. Chem. Rev.* **1995**, *140*, 137–168.
(18) (a) Chevrier, B.; Diebold, T.; Weiss, R. *Inorg. Chim. Acta* **1976**, *19*, L57–L59. (b) Ledon, H.; Bonnet, M. *J. Chem. Soc., Chem. Commun.* **1979**, 702–704. (c) Mentzen, B. F.; Bonnet, M. C.; Ledon, H. J. *Inorg. Chem.* **1980**, *19*, 2061–2066.
(19) Hasegawa, K.; Imamura, T.; Fujimoto, M. *Inorg. Chem.* **1986**, *25*, 2154–2160.
(20) (a) Tachibana, J.; Imamura, T.; Sasaki, Y. *J. Chem. Soc., Chem. Commun.* **1993**, 1436–1439. (b) Tachibana, J.; Imamura, T.; Sasaki, Y. *Bull. Chem. Soc. Jpn.* **1998**, *71*, 363–369. (c) Fujihara, T.; Hoshiba, K.; Sasaki, Y.; Imamura, T. *Bull. Chem. Soc. Jpn.* **2000**, *73*, 383–390. (d) Fujihara, T.; Myougan, K.; Ichimura, A.; Sasaki, Y.; Imamura, T. *Chem. Lett.* **2001**, 186–187.
(21) Collman, J. P.; Kim, K.; Garner, J. M. *J. Chem. Soc., Chem. Commun.* **1986**, 1711–1713.
(22) *teXsan: Single-Crystal Structure Analysis Software*, Version 1.6; Molecular Structure Corp.: The Woodlands, 1993.
(23) Chang, C. K.; Abdalmuhdi, I. *J. Org. Chem.* **1983**, *48*, 5388–5390.

CH$_2$Cl$_2$ was discarded. The second red band eluted with 1% MeOH−CH$_2$Cl$_2$ (v/v) was collected, and the eluate was evaporated to dryness. The residue was dissolved again in a small amount of CH$_2$Cl$_2$ and crystallized by diffusion of MeOH. The resulting purple crystals were filtered, washed with MeOH, and dried under reduced pressure at 100 °C for 2 h. Yield: 30 mg (27%). Anal. Calcd for C$_{79}$H$_{83}$N$_8$O$_2$Mo: C, 74.57; H, 6.57; N, 8.81. Found: C, 73.70; H, 6.75; N, 8.78. UV−vis (CH$_2$Cl$_2$): λ_{max}/nm (ϵ/10^3 M^{-1} cm^{-1}) 345 (sh), 406 (136), 450 (55.8), 502 (14.1), 538 (8.52), 568 (16.0), 598 (5.81), 625 (2.78). ESR (CH$_2$Cl$_2$): g_{av} = 1.97, A_{Mo} = 46 × 10^{-4} cm^{-1}, A_N = 2.24 × 10^{-4} cm^{-1}. IR (KBr): ν/cm^{-1} 902 ($\nu_{Mo=O}$), 478 (ν_{Mo-O}), 3296 (ν_{N-H}). FAB-MS: m/z^+ = 1242 ([H$_2$(DPA)-(MoO)]$^+$).

(DPA)[Mo^{V}O(OMe)][Zn^{II}(MeOH)] (2). Method 1. A 30 mg sample of Zn(OAc)$_2$·2H$_2$O in MeOH (5 mL) was added to a solution of **1** (30 mg, 2.3 × 10^{-5} mol) in CH$_2$Cl$_2$ (50 mL). After the reaction mixture was refluxed for 30 min, the resulting solution was evaporated to dryness. The residue was again dissolved in CH$_2$Cl$_2$ followed by filtration to remove excess Zn(OAc)$_2$. The filtrate was passed through an alumina column (neutral, activity III, 2 × 10 cm). The first fraction eluted with CH$_2$Cl$_2$ was collected, and the eluate was evaporated to dryness. The residue was dissolved again in a small amount of CH$_2$Cl$_2$ containing MeOH (ca. 2%) and crystallized by diffusion of *n*-pentane. The obtained purple crystals were washed with *n*-pentane and dried under reduced pressure at 100 °C for 4 h. Yield: 25 mg (79%). Anal. Calcd for C$_{80}$H$_{85}$N$_8$O$_3$MoZn: C, 70.24; H, 6.26; N, 8.19. Found: C, 69.25; H, 6.46; N, 8.07. UV−vis (0.5% MeOH−CH$_2$Cl$_2$): λ_{max}/nm (ϵ/10^3 M^{-1} cm^{-1}) 341 (81.1), 414 (249), 458 (41.4), 545 (16.8), 575 (16.9), 598 (4.7). ESR (CH$_2$Cl$_2$): g_{av} = 1.97, A_{Mo} = 43 × 10^{-4} cm^{-1}, A_N = 2.43 × 10^{-4} cm^{-1}. IR (KBr): ν/cm^{-1} 916 ($\nu_{Mo=O}$), 428 (ν_{Mo-O}). FAB-MS: m/z^+ = 1304 ([(DPA)(MoO)Zn]$^+$).

Method 2. H$_2$(DPA)[Zn][14] (50 mg, 4.2 × 10^{-5} mol) and an excess of Mo(CO)$_6$ (100 mg, 3.8 × 10^{-4} mol) were added to the mixed solvent of decalin (36 mL) and *n*-octane (9 mL). The mixture was refluxed for 2 h under N$_2$, cooled, and filtered. The filtrate was passed through an alumina column (neutral, activity III, 2 × 10 cm). The first red band, which was eluted with 1% MeOH−CH$_2$Cl$_2$ (v/v), was collected, and the eluate was evaporated to dryness. The residue was dissolved again in a small amount of CH$_2$Cl$_2$ containing MeOH (ca. 2%) and crystallized by diffusion of *n*-pentane. The purple crystals obtained were washed with *n*-pentane and dried under reduced pressure at 100 °C for 4 h. Yield: 26 mg (47%).

Mo^{V}O(MPP)(OMe) (3). H$_2$MPP (200 mg, 3.6 × 10^{-4} mol) and an excess of Mo(CO)$_6$ (200 mg, 7.6 × 10^{-4} mol) were added to the mixed solvent of decalin (36 mL) and *n*-octane (9 mL). The mixture was refluxed for 2 h under N$_2$, cooled, and filtered. The filtrate was passed through a silica gel column (Wakogel C-300HG, 2 × 20 cm). The first band eluted with CH$_2$Cl$_2$ contained the free-base porphyrin. The second green band eluted with 2% MeOH−CH$_2$Cl$_2$ (v/v) was collected, and the eluate was evaporated to dryness. The residue was dissolved in a small amount of CH$_2$Cl$_2$ and crystallized by diffusion of *n*-pentane. The brown-green powder was filtered, washed with *n*-pentane, and dried under reduced pressure at 100 °C for 2 h. Yield: 87 mg (34%). Anal. Calcd for C$_{44}$H$_{28}$N$_4$O$_3$Mo: C, 67.33; H, 6.23; N, 8.05. Found: C, 67.10; H, 6.42; N, 8.08. UV−vis (CH$_2$Cl$_2$): λ_{max}/nm (ϵ/10^3 M^{-1} cm^{-1}) 345 (49.3), 446 (87.3), 564 (15.6), 598 (5.77). ESR (CH$_2$Cl$_2$): g_{av} = 1.96, A_{Mo} = 43 × 10^{-4} cm^{-1}, A_N = 2.23 × 10^{-4} cm^{-1}. IR (KBr): ν/cm^{-1} 902 ($\nu_{Mo=O}$), 452 (ν_{Mo-O}). FAB-MS: m/z^+ = 666 ([MoO(MPP)]$^+$).

Scheme 1
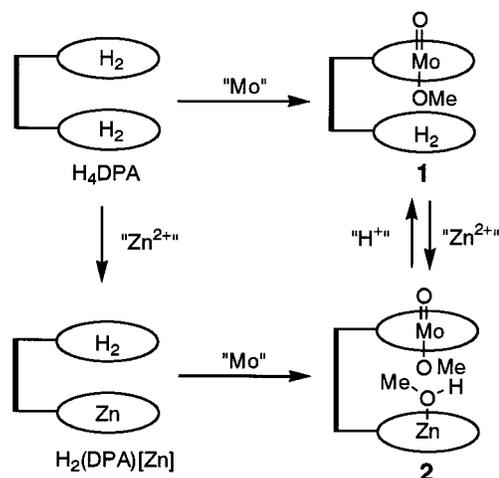
Zn^{II}(MPP) (4). H$_2$MPP in CH$_2$Cl$_2$ was treated with Zn(OAc)$_2$·2H$_2$O in MeOH to give Zn(MPP) quantitatively. Anal. Calcd for C$_{38}$H$_{40}$N$_4$Zn: C, 73.84; H, 6.52; N, 9.06. Found: C, 73.92; H, 6.71; N, 9.16. ^{1}H NMR (CDCl$_3$, 270 MHz): δ/ppm 10.16 (s, 2H, meso H), 10.06 (s, 1H, meso H), 8.08 (d, 2H, phenyl H), 7.75 (m, 3H, phenyl H), 4.05 (dq, 8H, CH$_2$CH$_3$), 3.65 (s, 6H, CH$_3$), 2.46 (s, 6H, CH$_3$), 1.90 (t, 6H, CH$_2$CH$_3$), 1.77 (t, 6H, CH$_2$CH$_3$). UV−vis (CH$_2$Cl$_2$): λ/nm (ϵ/10^3 M^{-1} cm^{-1}) 404 (424), 534 (18.1), 569 (17.3). FAB-MS: m/z^+ = 616 ([Zn(MPP)]$^+$).

Results and Discussion

Synthesis of DPA Complexes with an Oxomolybdenum(V) Unit. The outline of the syntheses of the DPA complexes of **1** and **2** is summarized in Scheme 1.[24] The insertion of molybdenum ion into H$_4$DPA was carried out using Mo(CO)$_6$ as a metal source. By changing both the reflux time and the amount of metal source, the mono-molybdenum porphyrin complex of **1** was successfully isolated.[25] The introduction of zinc(II) ion into the free-base porphyrin unit of **1** with Zn(OAc)$_2$·2H$_2$O gave **2**. **2** was also prepared from H$_2$(DPA)[Zn] as described in the Experimental Section.[11−15] In the preparation method, the monozinc complex of H$_2$(DPA)[Zn] was directly treated with Mo(CO)$_6$ to yield **2**. Successive treatments of **2** in CH$_2$Cl$_2$ with dilute HCl$_{aq}$ led to the monomolybdenum complex of **1**.

The elemental analyses of **1**−**4** were consistent with their respective compositions. The FAB-MS spectrum of **1** indicated that an oxomolybdenum unit was introduced into one of two porphyrin units in DPA. The insertion of a zinc ion was also confirmed by FAB-MS; that is, **2** showed the parent peak at 1304 (m/z^+), whereas **1** had the parent peak at 1242 (m/z^+).

1 and **2** showed characteristic ESR signals of oxomolybdenum(V) porphyrins, that is, six weak signals derived from ^{95,97}Mo (I = 5/2) and a strong signal due to the molybdenum

(24) Preliminary X-ray structure analysis of **1** showed that the oxo ion coordinated to the central molybdenum ion is directed to the outside of the dimer core; the same is true for **2**. The data will be reported somewhere after refinements.

(25) Another green band, which was eluted with 5% MeOH/CH$_2$Cl$_2$, was obtained. The FAB-MS spectrum for the solid material shows a peak at m/z^+ = 1351, which corresponds to bis(oxomolybdenum) DPA complexes. The characterization of the complex is now in progress.
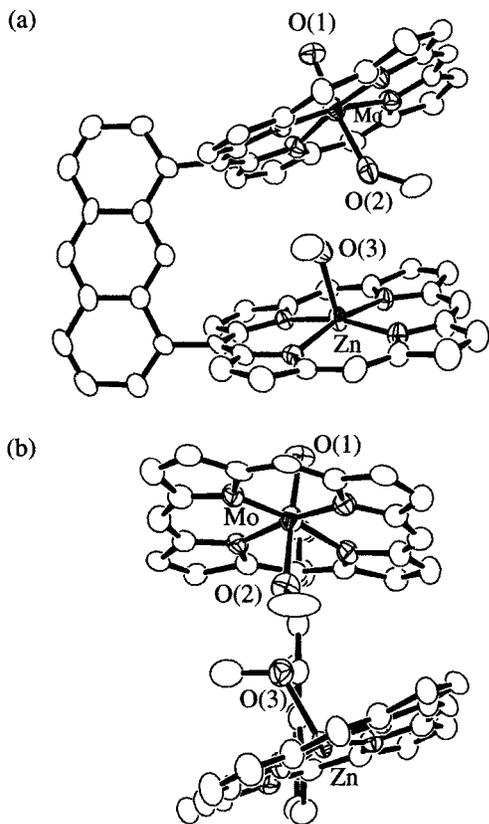
Figure 2. Molecular structure of **2**: (a) side view, parallel to the bridge plane; (b) side view, perpendicular to the bridge plane. Methy and ethyl groups of the DPA unit were omitted for clarity.

nucleus with $I = 0$. The strong signal splits into nine hyperfine lines because of the interaction with the four nitrogen nuclei ($I = 1$).[16] A corresponding monomeric complex of **3** also showed the characteristic ESR signals. These results clearly indicate that the valence states of molybdenum ion in **1**–**3** are +5.

Crystal Structure of (DPA)[Mo^{V}O(OMe)][Zn^{II}(MeOH)] (2). A crystal of **2** suitable for X-ray diffraction study was obtained by the diffusion of *n*-pentane into a CH$_2$Cl$_2$ solution of **2** containing a small amount of MeOH. Figure 2 shows the molecular structure of **2**. The selected bond lengths and bond angles around the central metal ions are listed in Table 2.

One of the porphyrin rings is metalated by a molybdenum ion and the other by a zinc ion. The molybdenum ion is hexacoordinated with an oxo and a methoxo ligand. Although there are two possible conformations of an oxo ligand bound to a molybdenum ion, that is, outside or inside the DPA unit, the crystal structure clarified that the terminal oxo ligand is positioned outside the DPA unit. The zinc ion is penta-coordinated by a methanol at the fifth position. Both the methoxo and methanol ligands are situated inside the DPA unit. The molybdenum porphyrin unit is oriented toward the outside, and the zinc porphyrin unit is largely bent with respect to the anthracene unit. Dihedral angles between the anthracene mean plane and each porphyrin mean plane of 24 atoms are 84.1° (Mo side) and 68.3° (Zn side). The dihedral angle between two porphyrin units is up to 31.8°.

Table 2. Selected Bond Lengths (Å) and Bond Angles (deg) of **2**

molybdenum unit		zinc unit	
bond	length/Å	bond	length/Å
Mo(1)−O(1)	1.722(6)	Zn(1)−O(3)	2.180(6)
Mo(1)−O(2)	1.993(6)	Zn(1)−N(5)	2.086(7)
Mo(1)−N(1)	2.065(6)	Zn(1)−N(6)	2.064(7)
Mo(1)−N(2)	2.090(7)	Zn(1)−N(7)	2.061(7)
Mo(1)−N(3)	2.090(7)	Zn(1)−N(8)	2.045(7)
Mo(1)−N(4)	2.069(8)		

molybdenum unit		zinc unit	
atoms	angle/deg	atoms	angle/deg
O(1)−Mo(1)−O(2)	172.3(3)	O(3)−Zn(1)−N(5)	89.2(2)
O(1)−Mo(1)−N(1)	98.2(3)	O(3)−Zn(1)−N(6)	97.7(3)
O(1)−Mo(1)−N(2)	91.6(3)	O(3)−Zn(1)−N(7)	103.1(3)
O(1)−Mo(1)−N(3)	89.9(3)	O(3)−Zn(1)−N(8)	96.6(2)
O(1)−Mo(1)−N(4)	96.2(3)	N(5)−Zn(1)−N(6)	90.1(3)
O(2)−Mo(1)−N(1)	89.0(2)	N(5)−Zn(1)−N(7)	167.7(3)
O(2)−Mo(1)−N(2)	85.7(3)	N(5)−Zn(1)−N(8)	88.6(3)
O(2)−Mo(1)−N(3)	82.9(3)	N(6)−Zn(1)−N(7)	87.7(3)
O(2)−Mo(1)−N(4)	86.5(3)	N(6)−Zn(1)−N(8)	165.6(3)
N(1)−Mo(1)−N(2)	92.3(3)	N(7)−Zn(1)−N(8)	90.5(3)
N(1)−Mo(1)−N(3)	171.9(3)		
N(1)−Mo(1)−N(4)	87.1(3)		
N(2)−Mo(1)−N(3)	87.4(3)		
N(2)−Mo(1)−N(4)	172.2(3)		
N(3)−Mo(1)−N(4)	92.1(3)		

The total feature of the structure of **2** is very similar to that of (DPA)[Ga(OMe)][Ru(MeOH)(CO)].[15]

The central molybdenum atom is displaced by 0.13 Å toward the oxo ligand from the mean plane of the 24-atom porphyrin core, and by 0.143 Å from the mean plane defined by the four nitrogen atoms. The bond lengths of Mo=O (1.722(6) Å) and Mo−N (average 2.08 Å) are in the range of those of oxomolybdenum(V) porphyrins with a monodentate axial ligand.[26,27] The Mo−O(OMe) distance (1.993(6) Å) is slightly longer than that observed in Mo^{V}O-(DPTBTMP)(OMe) (1.89(9) Å).[27] The longer distance must be due to the presence of the hydrogen bond between the methoxo ion and the methanol coordinated to the zinc ion (vide infra).

The zinc center of **2** adopts an approximate square-pyramidal geometry. The zinc atom is displaced by 0.23 Å toward the methanol ligand from the mean plane of the 24-atom porphyrin core, and by 0.24 Å from the mean plane of the four nitrogen atoms. Although the average Zn−N distance (2.06 Å) is comparable to those of pentacoordinated zinc(II) porphyrins with a methanol as an axial ligand,[28–30] the relatively short distance of Zn−O(MeOH) (2.180(6) Å) supports the presence of the hydrogen bond.[29]

(26) (a) Ledon, H. J.; Mentzen, B. *Inorg. Chim. Acta* **1978**, *31*, L393–L394. (b) Imamura., T.; Furusaki, A. *Bull. Chem. Soc. Jpn.* **1990**, *63*, 2726–2727. (c) Hamstra, B. J.; Cheng, B.; Ellison, M. K.; Scheidt, W. R. *Inorg. Chem.* **1999**, *38*, 3554–3561.

(27) van der Dijk, M.; Morita, Y.; Pertovic, S.; Sanders, G. M.; van der Plas, H. C.; Stam, C. H.; Wang, Y. *J. Heterocycl. Chem.* **1992**, *29*, 81–86.

(28) (a) Senge, M. O.; Kalisch, W. W. *Inorg. Chem.* **1997**, *36*, 6103–6116. (b) Barkigia, K. M.; Berber, M. D.; Fajer, J.; Medforth, C. J.; Renner, M. W.; Smith, K. M. *J. Am. Chem. Soc.* **1990**, *112*, 8851–8857.

(29) (a) Liang, Y.; Chang, C. K. *Tetrahedron Lett.* **1995**, *36*, 3817–3820. (b) Bag, N.; Chern, S-.S.; Peng, S-.M.; Chang, C. K. *Inorg. Chem.* **1995**, *34*, 753–756.

(30) Senge, M. O.; Eigenbrot, C. W.; Brennan, T. D.; Shusta, J.; Scheidt, W. R.; Smith, K. M. *Inorg. Chem.* **1993**, *32*, 3134–3142.

Table 3. Conformational Parameters for Cofacial Bisporphyrin Complexes

complex	Ct−Ct/Å[a]	M−M/Å	tilt/deg[b]	α/deg[c]	Sr/Å[d]	Sp/Å[e]	ref
(DPA)[MoO(OMe)][Zn(MeOH)] (**2**)	6.00	5.89	31.8	21.8	5.57	2.23	f
(DPA)[Ga(OMe)][Ru(MeOH)(CO)]	6.48	6.17	22.6	19.1	6.12	2.12	15
(DPA)[Ga(OMe)]₂	4.55	5.25	7.2	29.4	3.96	2.23	15
(DPA)[Ga(**μ**-OH)−Ru(CO)]	4.26	3.95	13.0	7.6	4.22	0.56	15
(DPA)[Ni]₂	4.56	4.57	2.4	31.7	3.87	2.39	31
(DPA)[Lu(OH)]₂·MeOH	5.67	3.52	19.7	14.1	5.49	1.39	32
(DPA′)[Fe₂(μ-im)(Him)₂]Cl	5.96	5.96	28.4	14.2	5.78	1.46	33
(DPB)[Co][Al(OEt)]	4.08	4.37	7.4	29.8	3.54	2.03	11
(DPB)[Cu][MnCl]	3.94	4.13	5.2	25.8	3.54	1.71	12

[a] The macrocycle center (Ct) was determined as the average position of the four nitrogens for each macrocycle. Ct−Ct is the distance between the two centers. [b] The angle (tilt) was calculated as the dihedral angle between the two 24-atom mean planes of the porphyrins. [c] The slip angle (α) was calculated as the average angle between the vector connecting the two "Ct" centers and the unit vectors normal to the two macrocyclic 24-atom mean plane; that is, $\alpha = (\alpha_1 + \alpha_2)/2$. [d] The inter-ring separation was defined as $Sr = (Ct-Ct)\cos\alpha$. [e] The slip parameter was determined as $Sp = (Ct-Ct)\sin\alpha$. [f] This work.
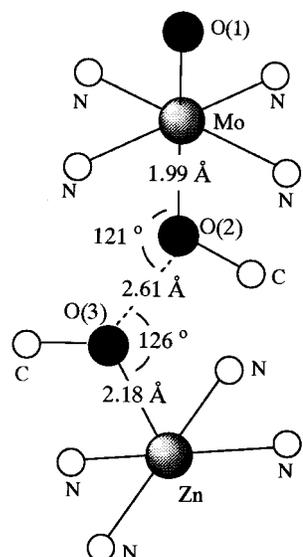
Figure 3. Diagram illustrating the coordination environment of **2**.

Figure 4. UV−vis spectra of **1** (a) and the relevant monomer compounds (b) in CH₂Cl₂ at room temperature: dashed line, **3**; dotted line, H₂MPP; solid line, calculated sum of two spectra.

It is interesting that a methanol exists inside the DPA cavity, though the inside of the DPA pocket is sterically crowded. The distance between the oxygen atom (OMe) coordinated to the molybdenum(V) ion and that (MeOH) to the zinc(II) ion is 2.61 Å as illustrated in Figure 3. The short contact between the two oxygen atoms also supports the presence of the hydrogen bond. The angles Mo−O(2)−O(3) and Zn−O(3)−O(2) are 120.9(2)° and 126.4(3)°, respectively. The hydrogen atom must locate on the line between two oxygen atoms, though the X-ray analysis was not able to determine the position accurately. The reason the methanol is captured inside the DPA cavity is that the methanol ligand is stabilized by both the coordination bond and the hydrogen bond. This result does not contradict with the data of Zn(5-NO₂-OEP)(MeOH), in which the intermolecular O−O distance of two methanols coordinated to two adjacent zinc(II) ions is 2.83 Å.[30]

Table 3 summarizes several parameters of the structure and the conformation of the diporphyrin complexes.[11,12,15,31−33] In the homometallic diporphyrins of the lutetium(III)[32] and iron(III)[33] complexes, the distortions are symmetrical with respect to the two porphyrin units, or take the simple open conformation of the DPA unit. In contrast, asymmetrical structures appear to be specific for the heterometallic diporphyrins of **2** and (DPA)[Ga(OMe)][Ru(MeOH)(CO)][15] having a methoxo ion and a methanol in the pocket; that is, the two porphyrin rings are open and distorted asymmetrically. Both the diporphyrins also have a large center-to-center distance (6.00 Å for **2** and 6.48 Å for (DPA)[Ga(OMe)]-[Ru(MeOH)(CO)]).

Infrared and UV−Vis Spectroscopy. **1** gives the IR bands of Mo=O and Mo−O at 902 and 478 cm⁻¹, respectively. These values are comparable to the stretching of oxomolybdenum(V) porphyrins having an alkoxo ligand,[16] and those of **3**. **1** also shows a weak absorption band due to inner NH stretching of the free-base porphyrin unit at 3296 cm⁻¹. In the case of **2**, the band of Mo−O stretching (428 cm⁻¹) is shifted by 50 cm⁻¹ to lower wavenumbers compared to that of **1**. This shift must result from the formation of the

(31) Fillers, J. P.; Ravichandran, K. G.; Abdalmuhdi, I.; Tulinsky, A.; Chang, C. K. *J. Am. Chem. Soc.* **1986**, *108*, 417−424.
(32) Lachkar, M.; Tabard, A.; Brandes, S.; Guilard, R.; Atmani, A.; De Cian, A.; Fischer, J.; Weiss, R. *Inorg. Chem.* **1997**, *36*, 4141−4146.
(33) Naruta, Y.; Sawada, N.; Tadokoro, M. *Chem. Lett.* **1994**, 1713−1716.
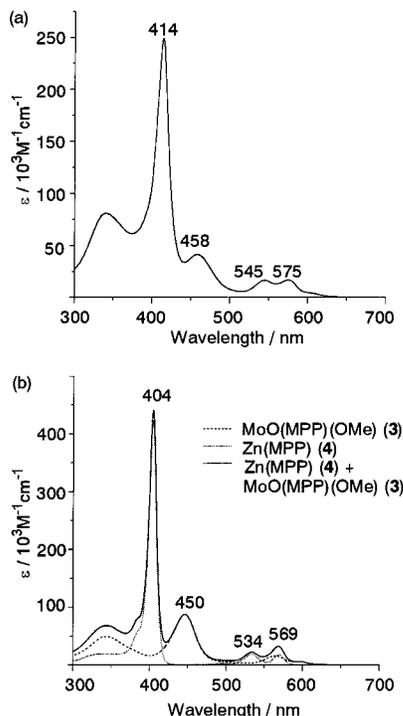
Figure 5. UV−vis spectra of **2** (a) and the relevant monomer compounds (b) in 0.5% MeOH−CH$_2$Cl$_2$ at room temperature: dashed line, **3**; dotted line, **4**; solid line, calculated sum of two spectra.

Figure 6. Cyclic voltammograms of **2** in 0.1 M TBAP−CH$_2$Cl$_2$. The oxidation process was displayed in the potential ranges −1.0 to +1.3 V (a) and −1.0 to +1.6 V (b). The reduction process was shown in the potential range +0.2 to −1.5 V (c).

Scheme 2

hydrogen bond between the methoxo ligand and the methanol ligand, as found in the crystal structure.

Figure 4a shows a UV−vis spectrum of **1** in CH$_2$Cl$_2$. Although **1** has many absorption bands at 345, 406, 450, 502, 538, 568, 598, and 625 nm, the spectrum was clearly analyzed as the overlap of those of **3** and H$_2$MPP. **3** has absorption bands at 345, 446, 564, and 598 nm, and H$_2$MPP at 402, 501, 535, 570, and 623 nm, as shown in Figure 4b. The result suggests that there are few interactions between the two porphyrin units.

The UV−vis spectrum for the CH$_2$Cl$_2$ solution of **2** at concentrations lower than 5×10^{-6} M shows the Soret band of the zinc porphyrin unit at 407 nm. However, by an increase in the concentration to ca. 10^{-4} M or by the addition of 0.5% MeOH to the solution at low concentrations, the Soret band red-shifted to 414 nm (Figure 5a). This spectrum is different from the superposition of the components of **3** and **4** (Figure 5b). Since the red shift of the Soret band of zinc(II) porphyrins is generally observed by the coordination of bases such as pyridine, the UV−vis spectrum for high concentrations of **2** in solution is explained by the coordination of a methanol to the zinc(II) porphyrin. In **4** itself, the addition of the same amount of MeOH to the CH$_2$Cl$_2$ solution caused no red shifts. Thus, the relatively stable coordination of methanol to zinc(II) ion must be specific to **2**.[34]

Electrochemistry. The redox behavior for ca. 1×10^{-3} M mixed-metal complex of **2** is summarized in Scheme 2. The voltammograms of **2** in three different potential ranges

are displayed in Figure 6. In the potential range between 0 and +1.2 V in Figure 6a, two reversible oxidation peaks were observed at +0.49 and +0.96 V ($E_{1/2}$ = half-wave potential). These peaks (I and II) are due to the formation of the monocation and dication radicals of the zinc(II) porphyrin unit, respectively, as compared to **4**. Remarkably, the first oxidation process of **2** to form monocation radical shows a large negative shift (ΔE = 180 mV), in comparison to the oxidation of **4** at +0.67 V ($E_{1/2}$), due to the coordination of methanol to the zinc(II) ion.[35] When the potential was scanned positively up to +1.6 V as shown in Figure 6b, another reversible oxidation peak was observed at +1.47 V ($E_{1/2}$, peak III), which was assigned to the ring-centered oxidation of the molybdenum porphyrin unit.

The negative scan from the potentials over +0.96 V gave two small reduction peaks at around +0.6 and −0.2 V aside

---

(34) Although the UV−vis spectrum of **2** showed the Soret band at 414 nm at concentrations higher than 10^{-4} M in neat CH$_2$Cl$_2$, the determination of the molar absorptivity of **2** was performed for a solution containing 0.5% (v/v) MeOH to get accurate values.

(35) For the first oxidation of Zn(TPP)(L) (L = nitrogenous base) in CH$_2$Cl$_2$ containing 0.1 M TBAP and 1.0 M ligand, the half-wave potentials are in the narrow range of +0.74 to +0.83 V vs SCE. In this system, the values are not so different from that (+0.78 V) of Zn(TPP) without axial ligands. Kadish, K. M.; Shiue, L. R.; Rhodes, R. K.; Bottomley, L. A. *Inorg. Chem.* **1981**, *20*, 1274−1277.

from the peak at −0.78 V (Figure 6b). Since [Zn^{II}(MPP)]$^+$ in **4** is reduced at +0.67 V and the Mo^{V}O(MPP)ClO$_4$ complex prepared independently has a reversible reduction peak of Mo(IV)/Mo(V) at −0.2 V, the two peaks at around +0.6 and −0.2 V in **2** should be ascribed to the ring-centered reduction of the zinc porphyrin unit without methanol ligands and the reduction of the Mo(IV)/Mo(V) of the molybdenum porphyrin unit without methoxo groups, respectively. When potentiostatic electrolysis of **2** was carried out at around +1 V followed by negative scans, the two peaks at +0.6 and −0.2 V increased in intensity with the increase of the electrolysis time. The results indicate that by the oxidation of **2** at the potentials over +0.96 V, both the methoxo ligand and the methanol ligand are in some amounts released from each metal ion.

In the direct negative scan in the potential range of +0.2 to −1.5 V, a reversible reduction peak (peak IV, $E_{1/2} = -0.78$ V) was observed as shown in Figure 6c. ESR measurements revealed that by the potentiostatic electrolysis of **2** at −1.0 V the characteristic ESR signal of the Mo(V) unit decreased in intensity, indicating the formation of a diamagnetic Mo(IV) porphyrin unit. The CV wave at −0.78 V is significantly different from that of the monomer system of Mo^{V}O(TPP)OMe, which gave an irreversible reduction peak.[36] The irreversibility of Mo^{V}O(TPP)OMe is owed to the release of the methoxo ligand after the reduction of the molybdenum(V) ion.[36] In the system of **2**, the repeated

positive scan gave almost the same oxidation peaks as the first one. The appearance of the reversible peak at −0.78 V in the system of **2** indicates that both the methoxo ligand and the methanol ligand are still coordinated to each metal ion even after the reduction. The two ligands must be sustained with the help of the DPA pocket and the hydrogen bond.

Conclusion

Novel anthracene-bridged porphyrin dimers having an oxomolybdenum(V) unit, H$_2$(DPA)[Mo^{V}O(OMe)] (**1**) and (DPA)[Mo^{V}O(OMe)][Zn^{II}(MeOH)] (**2**), and the relevant monomer complexes of Mo^{V}O(MPP)OMe (**3**) and Zn^{II}(MPP) (**4**) were synthesized and characterized. The structure of the mixed-metal complex of **2** was determined by X-ray crystallographic analysis. The results clearly indicate that a methanol molecule stably exists inside the DPA pocket due to both the coordination to the zinc(II) ion and the hydrogen bond with the methoxo ion. The UV−vis and cyclic voltammetric measurements of **2** suggest that the structure is retained even in solution. The study of other mixed-metal complexes having redox-active metal ions is now in progress.

Supporting Information Available: X-ray crystallographic data of **2** in CIF format and figures showing the full ORTEP drawing and schematic diagrams of perpendicular displacement of porphyrin cores of **2**. This material is available free of charge via the Internet at http://pubs.acs.org.

(36) (a) Kadish, K. M.; Malinski, T.; Ledon, H. J. *Inorg. Chem.* **1982**, *21*, 2982−2987. (b) Malinski, T.; Hanley, P. M.; Kadish, K. M. *Inorg. Chem.* **1986**, *25*, 3229−3235.

IC010323B